ARTICLE

NSG mice as hosts for oncological precision medicine

Claudia Maletzki [1] · Stephanie Bock[2] · Philipp Fruh[2] · Karolis Macius[2] · Anika Witt[2] · Friedrich Prall[3] ·
Michael Linnebacher[2]

Abstract

Patient-derived xenograft (PDX) models have been rediscovered as meaningful research tool. By using severely immunodeficient mice, high-engraftment rates can be theoretically achieved, permitting clinical stratification strategies. Apart from engraftment efficacy, tolerability towards certain cytostatic drugs varies among individual mouse strains thus impeding large-scale screenings. Here, we aimed at optimizing an in vivo treatment schedule using the widely applied cytostatic drug 5-fluoruracil (5-FU) for exemplary response prediction in colorectal cancer (CRC) PDX models. Four different individual CRC PDX models were engrafted into NOD.Cg-Prkdc^{scid}Il2rg^{tm1}Wjl (NSG) mice. Mice with established PDX were allocated to different treatment groups, receiving 5-FU, the oral prodrug Capecitabine, or 5-FU/leucovorin (LV) at different doses. Body weight, tumor size, and general behavior were assessed during therapy. Ex vivo analyses were done from blood samples, liver, as well as tumor resection specimen. Engraftment efficacy was high as expected in NSG mice, yielding stable PDX growth for therapy stratification. However, overall tolerability towards 5-FU was unexpectedly low, whereas the prodrug Capecitabine as well as the combination of 5-FU/LV at low doses were well tolerated. Accompanying plasma level determination of DYPD, the rate-limiting enzyme for 5-FU-mediated toxicity, revealed reduced activity in NSG mice compared with other common laboratory mouse strains, offering a likely explanation for the drug incompatibility. Also, the De Ritis quotient was highly elevated in treated mice, reflecting overall organ injury even at low doses. Summarizing these findings, NSG mice are ideal hosts for in vivo engraftment studies. However, the complex immunodeficiency reduces tolerance to certain drugs, thus making those mice especially sensitive. Consequently, such dose finding and tolerance tests constitute a necessity for similar cancer precision medicine approaches.

Introduction

Patient-derived xenograft (PDX) models have significantly improved basic and translational research. Direct xenografting of human cancerous tissue allows faithful resemblance of the patients' tumors with regard to histopathology, tumor microenvironment, gene expression, mutational status, and inflammation [1]. Also, high-throughput screening can be done to assess bioavailability, pharmacokinetic, and toxicity profile of clinically approved drugs/combinations and—even more important—novel drugs [2, 3].

Prior to performing in vivo drug response studies, selection of an appropriate immunodeficient mouse strain is recommended [4]. Several strains are available, with competing advantages and limitations when considering the rational design of therapy [1]. Athymic Foxn1^{nu} mice constitute the "classical" hosts enabling simple injection or implantation of foreign tumor material due to acomia and ease of handling. T cell deficiency enables engraftment with varying efficacy. In addition to the type and quality of the tumor used for xenografting, remnant immune function provides an obstacle, often resulting in poor engraftment efficiency. SCID (severe combined immunodeficiency), NOD-SCID (Nonobese diabetic-SCID), and recombination-activating gene 2 (Rag2)-knockout mice are other commonly used strains; albeit still primarily used to create xenografts using human cancer cell lines.

Primary patient-derived tumors require higher immuno-deficiency levels for good engraftment rates, avoiding

✉ Michael Linnebacher
  michael.linnebacher@med.uni-rostock.de

1 Department of Medicine, Clinic III-Hematology/Oncology/
   Palliative Care Rostock, Rostock, Germany

2 Molecular Oncology and Immunotherapy; Department of General
   Surgery, Rostock, Germany

3 Institute of Pathology, University Medical Centre, 18057
   Rostock, Germany

xenograft rejection as well as enabling sufficient PDX growth kinetics for subsequent therapy trials. NOD.Cg-Prkdc^{scid}Il2rg^{tm1}Wjl (NSG) mice lack T, B, functional NK cells as well as both alleles of the IL2 receptor common gamma chain, thus lacking cytokine signaling through multiple receptors. NSG mice were described to be lymphoma-resistant, providing a major advantage compared with other immunodeficient mouse strains, in which spontaneous lymphomagenesis is frequent [5, 6]. The severe immunodeficiency of NSG mice additionally allows successful humanization using human CD34^{+} hematopoietic stem cells, peripheral blood mononuclear cells or adult stem cells; and tumor tissues engraft to high frequencies [7, 8]. Hence, NSG is currently the only available mouse strain in which reconstitution of the human immune system, including functional T cell responses has been described. While creating an environment that guarantees full compatibility between the graft and the host, clinical responses to novel (immuno-) therapeutic interventions can be monitored. This is likely to be realized when malignant and immune cells are used from the same donor [9].

NSG mice principally meet all requirements for research addressing immune function, infectious disease, diabetes, stem cell biology, and oncology. The latter is an increasingly growing research field inspired by deeper knowledge of tumor biology and molecular pathology. PDX may guide the way to precision medicine shortly, i.e., "the right drug, for the right patient, at the right time" [6].

The first-line cytostatic agent for adjuvant treatment of colorectal cancer (CRC) patients is the antimetabolite 5-fluoruracil (5-FU), applied as single substance, its inactive prodrug Capecitabine or in combination with other cytostatics, such as oxaliplatin and irinotecan [10]. Upon application, 5-FU is metabolized intracellularly to several active metabolites (fluorodeoxyuridine monophosphate, fluorodeoxyuridine triphosphate, and fluorouridine triphosphate). These exert anticancer effects via two main mechanisms: (I) inhibition of thymidylate synthase (TYMS) and (II) incorporation into RNA and DNA. However, 5-FU response rates vary owing to the tumors' molecular heterogeneity and (still) poorly defined mechanisms of drug efficacy and resistance [11, 12].

Given these facts, a comprehensive in vivo study to accurately predict 5-FU response is indicated. This challenging question may be best answered in a PDX clinical trial (PCT), with a "one animal per model per treatment" experimental design [13]. The predictive value of such a trial is reliant on high-engraftment efficacy and tumor outgrowth within an appropriate time. NSG mice are thus the favored host. Prior to performing such a PCT, determining the best dose and treatment schedule with tolerable side effects and an optimal response is desirable. Hence, we here aimed to optimize in vivo doses of 5-FU in NSG mice harboring CRC PDX of different molecular subtypes to reflect the clinical situation at best.

Methods

Human cell lines and treatment schedule

The patient-derived CRC cell lines HROC24, HROC370 (both microsatellite instable; MSI), HROC40, HROC43 (both CpG island methylation phenotype; CIMP), HROC46 T0 M1, and HROC222 T1 M2 (both chromosomal instable; CIN) were established in our lab directly from patient material or after in vivo xenografting (nomenclature: HRO—Hansestadt Rostock; C—Colon; T—transfer; M—mouse; Table 1). Analyses were done on passages < 40. Cells were maintained in complete medium: DMEM/F12 supplemented with 10% fetal calf serum, glutamine (2 mmol/l), and antibiotics (PAN-Biotech GmbH, Aidenbach, Germany). Cells were seeded in 96-well plates at a density of 1×10^4 cells/well and allowed to adhere overnight. Thereafter, cells were treated with increasing 5-FU doses for two 72 h cycles. IC$_{50}$ values were calculated upon crystal violet staining from at least three independent experiments in comparison to untreated controls.

Mice and tumor xenografting

Experiments were performed on female and male 6–8-week-old NSG mice ($n = 40$) weighting 16–25 g. Mice were bred in the animal facility of the Rostock University Medical Center and maintained in specified pathogen-free conditions. Animals were exposed to 12 h light/12 h darkness cycles and standard pellet food and water ad libitum. All experiments were performed according to the guidelines of the local animal use and care committee, also approving this study (Landesamt für Landwirtschaft, Lebensmittelsicherheit und Fischerei Mecklenburg-Vorpommern, permit number: LALLF M-V/TSD/7221.3-1-005/17). Tumor pieces were obtained from previously xenografted patients' tumors and subsequent cryopreservation as described [14]. Detailed information on the patients' tumors as well as clinicopathological information is given in Table 1. PDX in passage <5 were used to retain tumor microenvironment and thus warrant reliability of results. PDX were implanted subcutaneously into the animals' right flank under anesthesia (ketamine/xylazine, 90/6 mg/kg bw). Tumor specimens ($3 \times 3 \times 3$ mm) were soaked in 100 μL Matrigel (Corning, Kaiserslautern, Germany) for >10 min at 4 °C prior to xenografting. Tumor growth was regularly monitored and therapy was initiated upon tumor establishment (~6 mm diameter).

Table 1 Clinicopathological characteristics as well as patients' follow-up information

Lab ID HROC	Sex/age	Tumor type	Localization	T	N	Lk (n) +	Lk (n) Σ	M	G	R	L	V	UICC	Molecular subtype	Adjuvant therapy	Outcome
29	M/59	Adenocarcinoma	Hepatic (right) flexure	T3	N2	8	30	M1	G3	R0	L0	V1	IVa	Lynch syndrome	None	59 years[†]
40	M/69	Adenocarcinoma	Descending	T3	N1	2	18	M0	G3	R0	L1	V1	IIIb	CIMP-H	5-FU	Alive
46	M/65	Adenocarcinoma	Ascending	T3	N0	0	34	M1	G3	R2	L0	V1	IVa	spCIN	Capecitabine	67 years[†]
222	M/79	Adenocarcinoma	Transverse	T3	N0	0	13	M0	G2	R0	L0	V0	IIa	spCIN	None	Alive

CIMP-H CpG island methylator phenotype high, *spCIN* sporadic chromosomal instable, † indicated dead
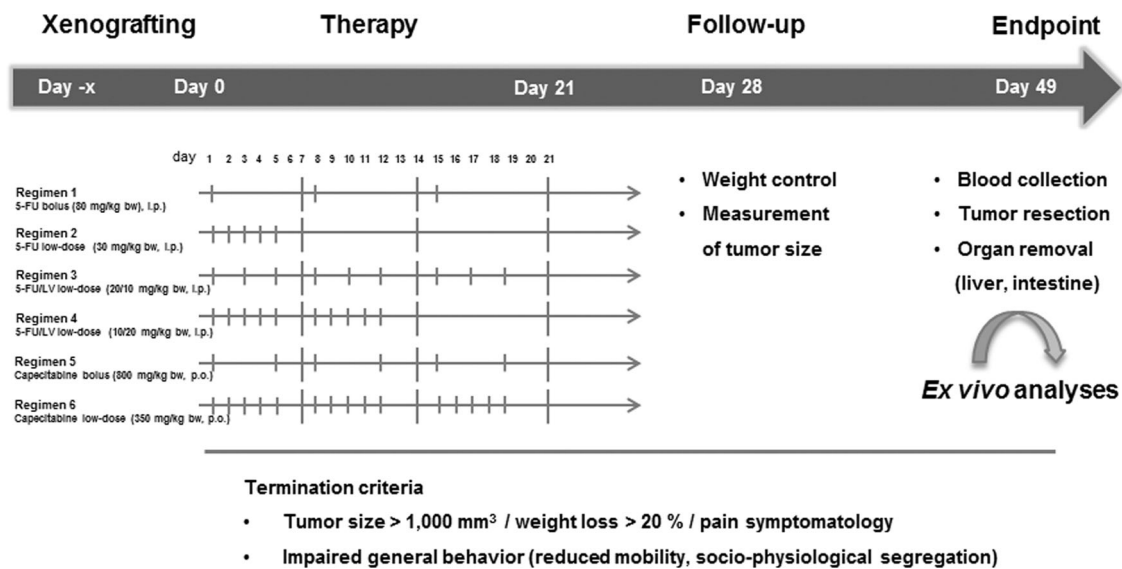

Fig. 1 Schedule of the experimental treatment protocol for dose optimization in vivo. NSG mice were implanted tumor tissue from individual CRC xenografts (size: $3 \times 3 \times 3$ mm, soaked in matrigel). Upon tumor establishment (~6mm), mice were divided into six treatment arms as shown (injection intervals are indicated by short vertical lines, long lines indicate weeks). Each group consisted of two mice. Follow-up was done by weekly weight control as well as tumor growth monitoring. The experimental endpoint was defined by excessive tumor growth (>1000 mm³) or impaired general behavior as stated in the figure. Ex vivo analyses were done as stated in material and methods

Treatment groups

Upon tumor establishment, mice were randomized into the following therapy groups with two animals/group (Fig. 1): (1) 5-FU bolus (80 mg/kg bw, intraperitoneal (i.p.), weekly, three times in total); (2) 5-FU low-dose (30 mg/kg bw, i.p. daily, five times in total); (3) 5-FU/leucovorin (LV) low-dose (20/10 mg/kg bw, i.p. thrice weekly, nine times in total); (4) 5-FU/LV low-dose (10/20 mg/kg bw, i.p. five times weekly, ten times in total); (5) Capecitabine bolus (800 mg/kg bw, peroral (p.o.), biweekly, six times in total); and (6) Capecitabine low-dose (350 mg/kg bw, p.o., five times weekly, 15 times in total). All mice received daily prepared soaked food during the experiments. Tumor growth and body weight were determined thrice weekly, to monitor any treatment-related toxicity. Mice were sacrificed after therapy completion, when they became moribund (weight loss >20% vs. start of therapy), when they exhibit impaired socio-physiological behavior, or when tumor sizes reached >1000 mm³. Blood samples as well as tumor tissues, liver, kidney, small, and large intestine were resected for further studies.

Dihydropyrimidine dehydrogenase (DYPD) ELISA

DYPD plasma levels were examined in untreated NSG mice ($n = 9$) and after therapy ($n = 2$). For comparison, plasma samples from wildtype C57Bl/6 J and Foxn1[nu] mice ($n = 3$ and 2, respectively) were also included into this analysis. DYPD levels were determined using a classical sandwich

Table 2 In vitro drug response analysis on selected patient-derived cell lines and comparison with in vivo growth pattern

Molecular subtype	Cell line	IC$_{50}$ 5-FU [μM]	Tumorigenic potential in vivo	Time of tumor outgrowth [d]	In vivo response
spMSI	HROC24	8	✓	23.0	Moderate[a]
	HROC370	4	✓	42.5	N.a.
spCIN	HROC46 T0 M1	8	✓	40.7	Moderate
	HROC222 T1 M2	**18**	✓	45.0	None
CIMP-H	HROC40	**22**	✓	50.6	Moderate
	HROC43	7	N.a.	N.a.	N.a.

5-FU sensitivity: high (italics)−low (bold)

spMSI sporadic microsatellite instable, *spCIN* sporadic chromosomal instable, *CIMP-H* CpG island methylator phenotype high

[a][16]

ELISA according to the manufacturers' instructions (Abbexa, Cambridge, UK).

Serum parameters

Blood samples were taken for spectrophotometric determination of plasma alanine aminotransferase (ALAT) and aspartate aminotransferase (ASAT) activities. Then, the *De Ritis quotient* was calculated by using the following formula: $\frac{ASAT}{ALAT}$ [15].

Histopathology

Immediately upon explantation, one half of the subcutaneous PDX tumor nodules was fixed in formalin and embedded in paraffin by routine procedures. H&E-stained sections (4 μm) were taken for light-microscopic study. Sections were assessed for morphologic features of therapy-induced tumor regression, namely necrosis, stromal fibrosis, and dystrophic calcifications.

Statistics

Statistical evaluation was performed using GraphPad PRISM software, version 5.02. Values are reported as the mean ± SD. After proving the assumption of normality *(D´Agostino & Pearson omnibus normality test)*, multiple comparisons were done by using one way ANOVA on ranks (Bonferroni's Multiple Comparison Test). The criterion for significance was taken to be $p < 0.05$.

Results

In vitro drug response analysis

5-FU responsiveness was first determined in vitro on a panel of patient-derived low-passage CRC cell lines. They were exposed to increasing drug concentrations (range: 0.49 μM–7.69 mM). Read out was done after two 72 h treatment rounds using crystal violet staining and IC$_{50}$ value determination.

The response profile was quite individual among cells (Table 2), nicely reflecting the heterogeneous clinical response towards 5-FU. Still, in vivo analysis is advisable for validation.

To prove 5-FU sensitivity in preclinical PDX models, four individual CRC cases were used which cover the percentual distribution of the CRC molecular subtypes, i.e., two cases from CIN tumors (HROC46 and HROC222), and one each with CIMP (HROC40) and MSI (HROC29) phenotype. Additional selection criteria were tumorigenic potential in vivo and tumor outgrowth within a reasonable time (Table 2).

In vivo dose-finding study

NSG mice carrying PDX from different CRC cases were initially treated with 30 mg/kg bw 5-FU (i.p. thrice weekly, nine times in total; $n = 4$ cases). Though tumor growth inhibition up to shrinkage was evident and thus largely confirmed in vitro findings, this dose was toxic to mice with unexpected death occurring in 4/4 PDX cases. Reducing 5-FU dose to 20 mg/kg bw, as described recently in another in vivo trial on 5-FU response towards HROC-PDX in NMRI Foxn1[nu] mice (namely HROC24), prevented toxicity [16]. However, dose-reduction abrogated therapeutic effects of 5-FU, with tumor growth curves similar to control mice *(data not shown)*. Consequently, we decided to systematically determine and thus optimize the 5-FU regimen to be used for subsequent studies in the NSG strain. More precisely, the best tolerated regimen(s) out of six different 5-FU applications with optimal therapeutic effects had to be identified. Mice with established PDX ($n = 4$ individual PDX models, namely HROC29, HROC40, HROC46, and HROC222, $n = 2$
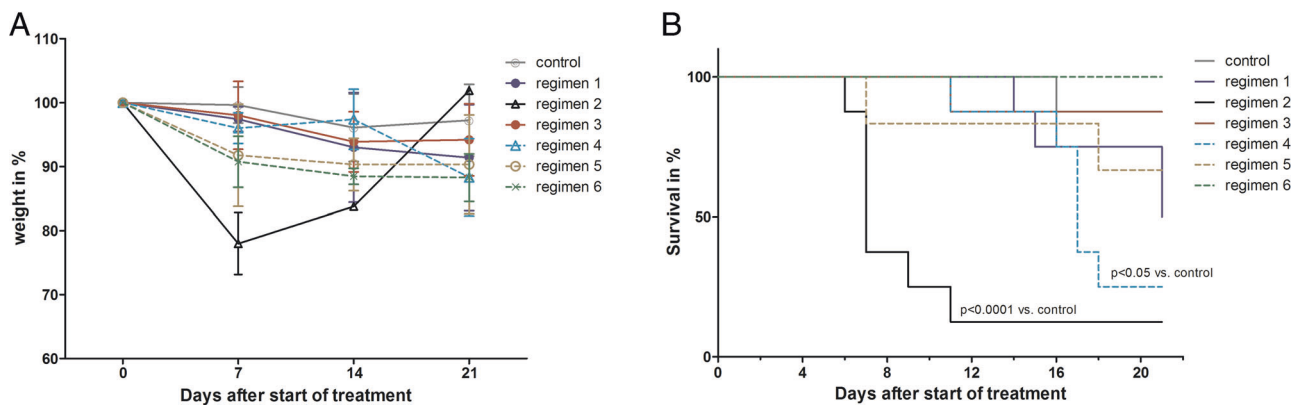
Fig. 2 Weight curve and survival analysis. **a** Body weight was checked thrice weekly and identified weight loss predominantly in the early phase of treatment, with recovery in most cases. Values are given as % weight vs. day $0 \pm$ SD; $n = 8$ mice per regimen, $n = 1$ control mouse/individual PDX case. **b** Kaplan–Meier survival curve analysis revealed changes between individual treatments, with highest treatment-related toxicity in regimen 2 independent of PDX case. $n = 8$ mice per regimen, $n = 1$ control mouse/individual PDX case. Significant differences between treatment and control mice are as follows: $p < 0.05$ regimen 4 vs. control; $p < 0.0001$ regimen 2 vs. control. One way ANOVA on ranks (Bonferroni's Multiple Comparison Test)

Table 3 Therapy-related and unexpected death in dose-optimization trial

Regimen	Deceased %		Median time of death [d]
	Treatment-related	Unexpected	
1	25.0	0.0	14
2	75	0.0	7
3	12.5	0	11
4	0.0	0.0	–
5	12.5	25	3
6	0.0	12.5	1.0

mice/group) were randomized into the six treatment groups (see Fig. 1 for details).

All treatment regimens were accompanied by transient weight loss (Fig. 2a), ruffling of fur and differing degree of diarrhea. Regimen 1 (5-FU bolus injection) exhibited low toxicity with 75% of mice surviving this therapy (Table 3 and Fig. 2b). Weight loss predominantly occurred 3–4 days after injection, with mice recovering afterwards (Fig. 2a). Regimen 2 (low-dose 5-FU) severely impaired state of health contributing to massive weight loss of affected mice (day 7: -23% vs. day 0). As a result, most mice died because of 5-FU-mediated toxicity within 1 week of treatment (Table 3 and Fig. 2b). The overall survival was only 25%. By contrast, the mice' general condition was not considerably impaired after treatment with 5-FU/LV (regimens 3 and 4) or Capecitabine (regimens 5 and 6), which was found to be favorable with regard to their side effects profile. In this latter regimen, weight changes were mainly seen at later time points (days 11–16), but persisted until the end of therapy (~10% vs. day 0) (Fig. 2a). 5-FU/LV

affected weight pattern only marginally, especially when given in low dose (regimen 4).

In vivo drug response

The in vivo drug response is shown in Fig. 3. Tumor sizes are standardized and given in percent of the respective control of each individual PDX case. The different toxicity profiles of the regimens were accompanied by individual treatment responses. Drug responses varied between regimens and PDX models from different molecular classes.

In detail, regimen 1 decelerated tumor growth the entire observation period in 3/4 cases (HROC29, HROC40, and HROC46) compared with the respective control groups ($p < 0.05$ vs. HROC222; Fig. 3). Due to differences in treatment response in the PDX model HROC40, tumor growth curves of this particular PDX are illustrated separately (Fig. 4a, tumor size as determined with a caliper).

In case of HROC222, no treatment response was observed at all; nicely confirming in vitro data (see Table 2). Regimen 2 impaired tumor growth in the two PDX models HROC40 and HROC46, but was accompanied by massive toxicity ($p < 0.05$ vs. HROC222; Fig. 2b). Tumor growth of all individual PDX models was marginally affected by regimen 3 and no treatment response was seen in regimen 4 (Fig. 3). We even observed a tendency towards an accelerated tumor growth (HROC40 at the beginning, HROC222 at later time points) in this particular treatment group. Regimens 5 and 6 slightly delayed tumor growth, with, however, individual differences.

By histological study, an effect of the various chemotherapeutic treatments was not seen in any of the PDX. Representative pictures taken from a control and 5-FU
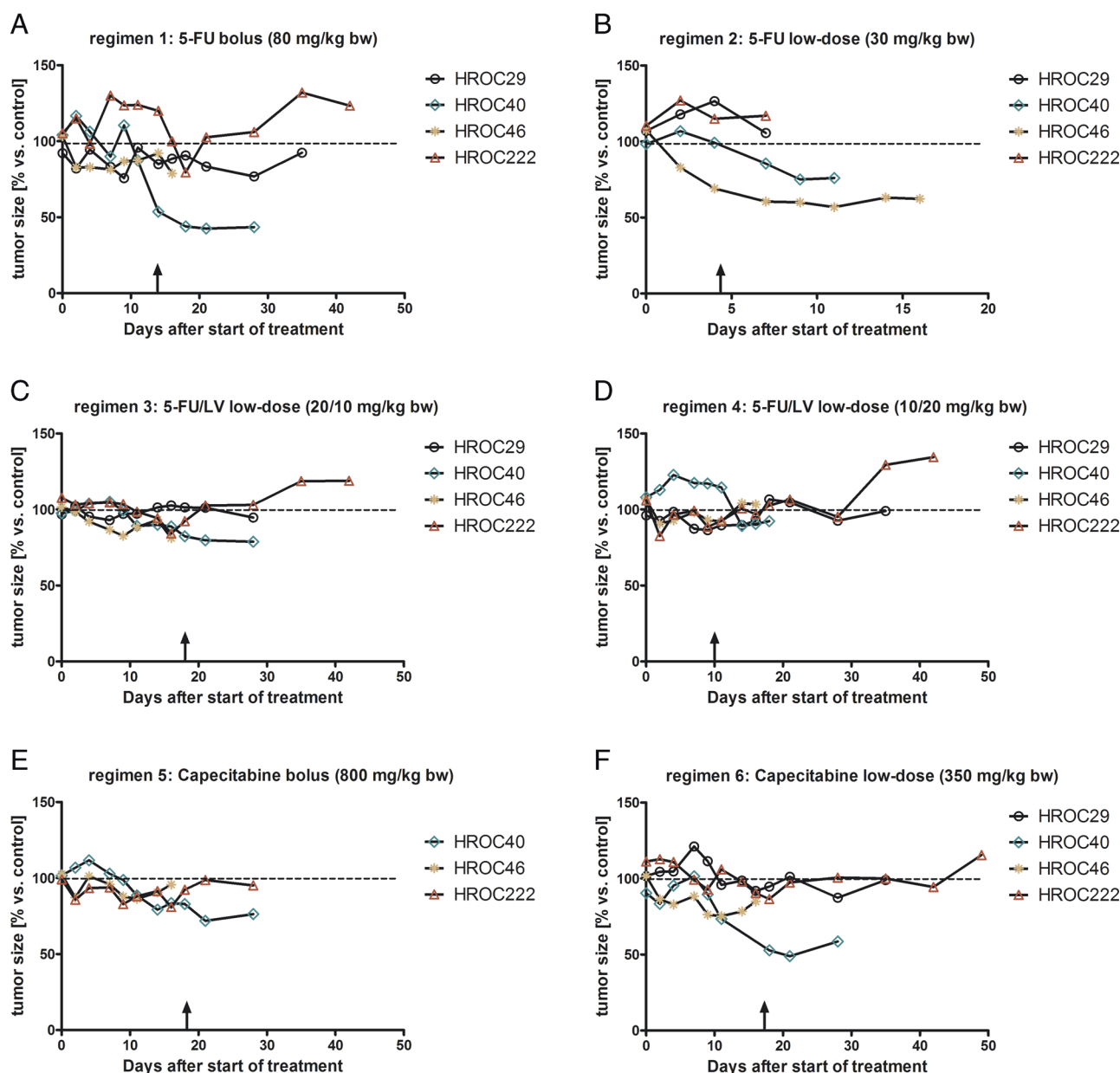
Fig. 3 Tumor growth curve. NSG mice with established PDX were treated as described in "Material and methods" section. Tumor size was measured thrice weekly using a caliper. Growth curves for each PDX case (namely HROC29, HROC40, HROC46, and HROC222) and treatment regimen is shown. Arrows indicate end of treatment. Values are given as % tumor size vs. tumor size of the corresponding control mouse (=untreated, set to be 100%); $n = 8$ mice per regimen, $n = 1$ control mouse/individual PDX case. Significant differences between individual PDX cases of each regimen include: regimen 1: $p < 0.05$ HROC222 vs. HROC29, HROC40, and HROC46; regimen 2/3: $p < 0.05$ HROC222 vs. HROC40 and HROC46; regimen 6: $p < 0.05$ HROC222 vs. HROC40 and HROC46; $p < 0.05$ HROC29 vs. HROC40 and HROC46; One way ANOVA on ranks (Bonferroni's Multiple Comparison Test)

treated PDX (case HROC40, regimen 6) are shown in Fig. 4b.

DYPD level and hematological changes upon therapy

Myelosuppression is a common side effect of 5-FU treatment, characterized by leukopenia and thrombocytopenia.

In this study, blood counts revealed only marginal hematological changes upon therapy. This was independent from the applied treatment regimen (*data not shown*) and most likely due to the complex immunodeficiency of NSG mice.

DYPD is the rate-limiting enzyme for pyrimidine base degradation and plays a pivotal role in 5-FU metabolism. Reduced DYPD activity due to gene polymorphism leads to severe toxicity following 5-FU injection in patients and

Fig. 4 **a** HROC40 PDX showing heterogeneous growth kinetic (slow vs. fast) within two mice and also different drug response. **b** Microscopic image of PDX HROC40. (Left) Control and (right) after 5-FU treatment. Note: Neoplastic gland invading the subcutaneous fat. However, just as in all other PDX, treatment effects were not observed
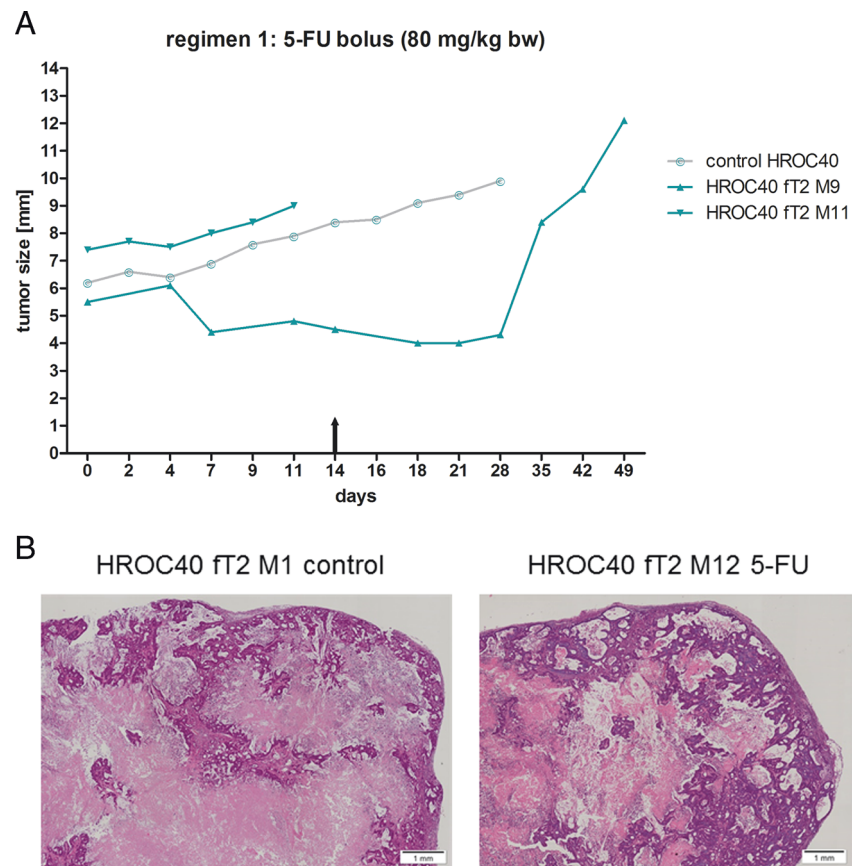
obliges individualized administration schemes [17]. Hence, we examined whether DYPD deficiency or low-expression level could explain the observed in vivo toxicity of high-dose 5-FU applications in NSG mice. By examining DYPD plasma levels using a classical ELISA assay in different standard laboratory mouse strains (NSG, C57Bl/6J, and NMRI Foxn1[nu]), variances became obvious (Fig. 5a). DYPD levels were significantly lower in NSG mice than in NMRI Foxn1[nu] mice ($p < 0.01$). Of note, we even identified additional reduction of the DYPD levels upon treatment, providing a likely explanation for the observed toxicity in NSG mice (Fig. 5a).

Analysis of plasma ALAT activities demonstrated no considerable differences between individual treatment groups as well as normal control values (Fig. 5b). However, ASAT activities were elevated in all treatment arms, with highest values observed in regimens 5 and 6 (Fig. 5c). Accordingly, the *De Ritis quotient* was highest in these two groups, reflecting overall organ injury upon treatment (Fig. 5d).

Discussion

Viability and sterility of tumor tissue are principal determinants for successful in vivo engraftment. Depending on the tumor origin (solid vs. hematological; primary vs. metastasis) and the mouse model used for engraftment, tumor take rates differ. Engraftment efficacy for CRC ranges between ~70% in NMRI Foxn1[nu] mice and ~80% in NSG mice [14] (*and own unpublished data*), providing a rationale for preferential use of NSG mice as hosts. Our lab possesses a huge collection of low-passage patient-derived CRC models to generate PDX from all currently known molecular subtypes [14, 16, 18–21]. Besides, this unique collection paves the way for a PCT to test candidate agents, helping to select effective treatments in a minimized number of animals [13]. The predictive value of preclinical trials in terms of clinical response is well-documented in literature [6, 22]. Different mouse strains were either engrafted with established cell lines (such as HCT116 or HT-29 for CRC) or with PDX for response prediction. Though not systematically addressed in literature, there is evidence of differential tolerability among individual mouse strains towards certain cytostatic drugs [23–25].

Thus, we here aimed to establish an effective treatment schedule with acceptable toxicity in NSG mice. 5-FU was chosen for drug response analysis on a basis of: (I) the broad clinical use for adjuvant and palliative therapy of different tumor entities, among them CRC; (II) the low level of side effects in clinical application, especially when given
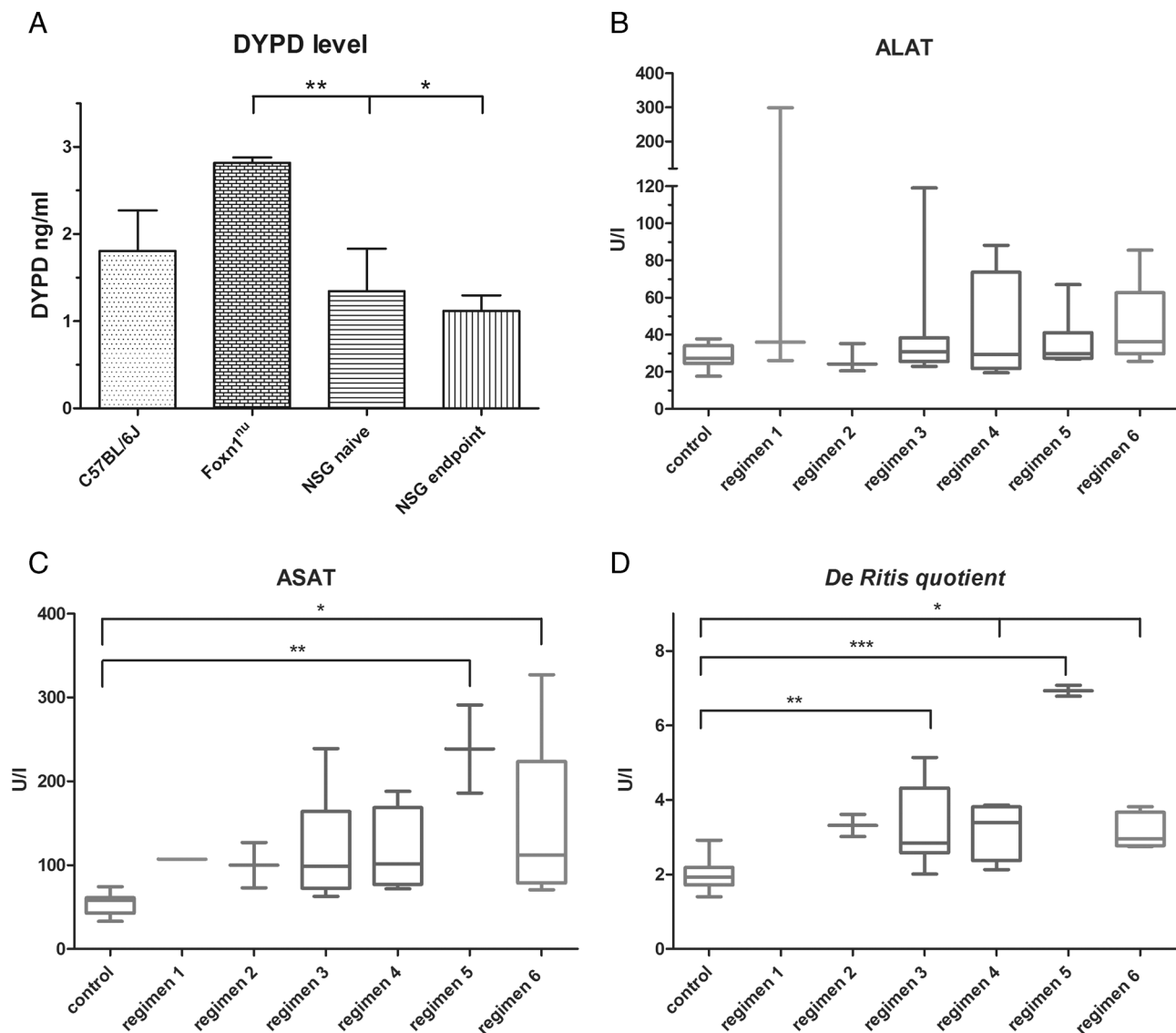
A

B

C

D

Fig. 5 In vivo and ex vivo analyses. **a** Basal plasma DYPD level revealed different between individual standard laboratory mouse strains. Values are given as mean ± SD. *$p < 0.05$ Foxn1[nu] vs. NSG endpoint; **$p < 0.01$ Foxn1[nu] vs. NSG naive; one way ANOVA on ranks. NSG mice ($n = 9$) and after therapy ($n = 2$). Plasma samples from wildtype C57Bl/6J and Foxn1[nu] mice result from $n = 3$ and 2 mice, respectively. **b–d** Plasma activity of liver enzymes **b** ASAT and **c** ALAT as well as the resulting **d** *De Ritis quotient* showing liver

injury upon therapy. Single measurement was done with plasma of $n = 1–7$ mice/regimen. $n = 12$ control mice. Values of are given as mean ± SD. Significant differences between individual regimens in comparison to controls are displayed in the graph. **b** *$p < 0.05$ regimen 6 vs. control and regimen 4 vs. control; **$p < 0.01$ regimen 3 vs. control; **d** ***$p < 0.0001$ regimen 5 vs. control. One way ANOVA on ranks (Bonferroni's Multiple Comparison Test)

as oral prodrug (=Capecitabine); and (III) synergism with other drugs (e.g., Irinotecan or Oxaliplatin) in combination regimens. 5-FU dose adjustment was done in compliance with guidelines for phase I clinical trials. Six different treatment regimens were applied.

Previous studies with NMRI Foxn1[nu] mice already described gradual weight loss as well as slight myelosuppression and gastrointestinal toxicity as most commonly seen 5-FU side effects [23–26]. Still, the heterogeneity in terms of (I) used mouse strains (NMRI Foxn1[nu] mice vs.

NSG mice); (II) tumor models (ectopic vs. orthotopic and syngeneic vs. xenograft); (III) the choice of treatment; and (IV) the chosen therapeutic regimen (weekly vs. daily, local vs. systemic application) hampers comparability of these previous studies. In our study, drug response and toxicity were quite heterogeneous, with an unexpectedly low tolerability towards half of the applied regimens.

Germline polymorphisms and resulting differences in terms of pharmacology between individual mouse strains may at least partly explain 5-FU-related toxicity. In men,

polymorphisms in the 5-FU converting enzyme DYPD are associated with reduced enzymatic activity or complete deficiency, present in ~3–5% of the general population [27]. It even constitutes a contraindication for 5-FU-based therapy due to the risk of potentially life-threatening toxicity, such as bone marrow suppression and neurotoxicity [27–30]. In mice, basal DYPD plasma levels significantly differed between the NMRI Foxn1^{nu} and NSG strains, with additional slight reductions of plasma DYPD upon 5-FU treatment in the latter. Of note, basal DYPD plasma level of NMRI Foxn1^{nu} mice exceeded those of another commonly used laboratory mouse strain (C57Bl/6J), providing a possible explanation for the in vivo toxicity present in NSG, but not in NMRI Foxn1^{nu} mice. Moreover, it is very likely that the complex immunodeficiency not only makes NSG mice particularly susceptible to 5-FU-based regimens, but it might also impact overall tolerability and response to other drugs. In a parallel unpublished study, the anthracycline topoisomerase inhibitor Doxorubicin was given at very low dose to leukemic NSG mice (PDX of different acute lymphoblastic leukemia [31]). However, all mice deceased within seven days of therapy (single or double i.p. application of 8 and 4 mg/kg bw, respectively, *own unpublished data*). With these results we back up the hypothesis that metabolisms are quite individual among laboratory animals. Though several studies hint towards gender-specific effects, we here provide, to the best of our knowledge, for the first time experimental evidence of mouse strain specific drug sensitivities. Keeping that in mind, the results of our systematic study lay ground for upcoming cancer precision medicine approaches aiming at validation of novel (potentially toxic) substances. In addition to the necessity of complex immunodeficiency, variations in pharmacogenetics among mice strains should be taken into consideration. We therefore strongly recommend performing a similar dose-finding prestudy to prevent unnecessary, expensive, and animal-consuming repetitive PCT with different drug regimens.

With regard to treatment efficacy, regimens 2, 5, and 6 tended to be best in the present study. Since regimen 2 was associated with severe toxicity, we cannot recommend this dosing schedule for future trials. Mice receiving regimens 5 and 6 were given Capecitabine orally. In support of clinical observations, this prodrug had antitumoral efficacy with low to moderate side effects in NSG mice. The observed increase in liver enzymes ASAT and ALAT in these two groups may be due to the higher local drug concentration, of note, without affecting mice' general condition.

By contrast, the addition of LV to 5-FU (therapy regimens 3 and 4) did not potentiate drug-mediated activity in vivo. In the clinic, LV is usually given after 5-FU infusion to reduce gastrointestinal toxicity and increase its efficacy. Here, we followed suggestions from a recent study

showing that simultaneous application of both substances is superior to sequential injection [32]. Functionally, effects were due to inhibited *TYMS* gene expression—the major target of 5-FU. Though not analyzed in detail, upregulation of *TYMS* instead of suppression might provide an explanation for treatment failure in our approach. This assumption is supported by in vitro findings, showing high upregulation of *TYMS* after single 5-FU exposure of CRC cells. Besides, *TYMS* is considered as another potential factor for drug-related toxicity [33]. But that has to be addressed prospectively.

Another challenge for PCT studies is the individual growth pattern of different PDX. Here, we selected PDX cases with stable engraftment efficacy (100%) and comparable growth kinetics. Still, in one case, an intrinsically decelerated growth pattern was seen, thus potentially biasing results. The different tumor development in case of HROC40 yielded conflicting outcomes with good response in one case showing slow tumor growth vs. no response in the other fast-growing tumor. This has to be considered while planning a PCT as well as analyzing obtained data afterwards.

Finally, we would like to emphasize that all treatment regimens were given after establishment of solid and clearly palpable tumors (~6–7 mm longitudinally). Virtually all PDX were allowed to grow for more than 40 days. In most studies documented in literature, therapy is started at earlier time with—in some cases—hardly visible tumors and resulting impressive growth inhibition. Still, the setting applied here better reflects the clinical situation of an advanced CRC and may explain our findings of only partial growth inhibition at best.

When comparing the clinical outcome of patients from which PDX were established with our in vitro findings, mixed results were obtained. All PDX models were generated from primary CRC cases representative for hereditary CRC (i.e., Lynch syndrome; HROC29), chromosomal instable CRC (HROC46 and HROC222), and CpG island methylator phenotype CRC (HROC40) [34]. Two patients presented with synchronous liver metastases at time of resection; one of them died immediately after surgery (HROC29; UICC IV). The second patient received palliative chemotherapy with Capecitabine, but deceased soon after (HROC46; UICC IV). The remaining two cases were staged lower according to the UICC system. One patient received 5-FU-based treatment (HROC40; UICC IIIa) and the other one no adjuvant therapy (HROC222; UICC IIa) in line with clinical recommendations for these UICC stages. Both patients are still alive (follow-up of 142 and 81 months, respectively). Although definitely not a primary endpoint of the current study, we want to emphasize the fact that the PDX treatment results of HROC40 and HROC46 very well correspond with the clinical course.

Data availability

Compliance with ethical standards

Conflict of interest The authors declare that they have no conflict of interest.

Ethical approval and consent to participate Specimen collection was conducted in accordance with the ethics guidelines for the use of human material, approved by the Ethics Committee of the University of Rostock (Reference numbers: II HV 43/2004 and A 45/2007) and with informed written consent from all patients prior to surgery.

Publisher's note: Springer Nature remains neutral with regard to jurisdictional claims in published maps and institutional affiliations.

References

1. Lai Y, Wei X, Lin S, Qin L, Cheng L, Li P. Current status and perspectives of patient-derived xenograft models in cancer research. J Hematol Oncol. 2017;10:106.
2. Meehan TF, Conte N, Goldstein T, Inghirami G, Murakami MA, Brabetz S, et al. PDX-MI: minimal information for patient-derived tumor xenograft models. Cancer Res. 2017;77:e62–6.
3. Byrne AT, Alférez DG, Amant F, Annibali D, Arribas J, Biankin AV, et al. Interrogating open issues in cancer precision medicine with patient-derived xenografts. Nat Rev Cancer. 2017;17:254–68.
4. Xu C, Li X, Liu P, Li M, Luo F. Patient-derived xenograft mouse models: a high fidelity tool for individualized medicine. Oncol Lett. 2019;17:3–10.
5. Mullins CS, Bock S, Krohn M, Linnebacher M. Generation of xenotransplants from human cancer biopsies to assess anti-cancer activities of HDACi. Methods Mol Biol. 2017;1510:217–29.
6. Jung J, Seol HS, Chang S. The generation and application of patient derived xenograft (PDX) model for cancer research. Cancer Res Treat. 2017;50:1–10.
7. Shultz LD, Brehm MA, Bavari S, Greiner DL. Humanized mice as a preclinical tool for infectious disease and biomedical research. Ann N Y Acad Sci. 2011;1245:50–4.
8. Zhou Q, Facciponte J, Jin M, Shen Q, Lin Q. Humanized NOD-SCID IL2rg –/– mice as a preclinical model for cancer research and its potential use for individualized cancer therapies. Cancer Lett. 2014;344:13–9.
9. Zitvogel L, Pitt JM, Daillère R, Smyth MJ, Kroemer G. Mouse models in oncoimmunology. Nat Rev Cancer. 2016;16:759–73.
10. Gustavsson B, Carlsson G, Machover D, Petrelli N, Roth A, Schmoll H-J, et al. A review of the evolution of systemic chemotherapy in the management of colorectal cancer. Clin Colorectal Cancer. 2015;14:1–10.
11. Rodrigues D, Longatto-Filho A, Martins SF. Predictive biomarkers in colorectal cancer: from the single therapeutic target to a plethora of options. Biomed Res Int. 2016;2016:6896024.
12. Devaud N, Gallinger S. Chemotherapy of MMR-deficient colorectal cancer. Fam Cancer. 2013;12:301–6.
13. Gao H, Korn JM, Ferretti S, Monahan JE, Wang Y, Singh M, et al. High-throughput screening using patient-derived tumor xenografts to predict clinical trial drug response. Nat Med. 2015;21:1318–25.
14. Linnebacher M, Maletzki C, Ostwald C, Klier U, Krohn M, Klar E, et al. Cryopreservation of human colorectal carcinomas prior to xenografting. BMC Cancer. 2010;10:362.
15. Peltenburg HG, Hermens WT, Willems GM, Flendrig JG, Schmidt E. Estimation of the fractional catabolic rate constants for the elimination of cytosolic liver enzymes from plasma. Hepatology. 1989;10:833–9.
16. Rohde S, Lindner T, Polei S, Stenzel J, Borufka L, Achilles S, et al. Application of in vivo imaging techniques to monitor therapeutic efficiency of PLX4720 in an experimental model of microsatellite instable colorectal cancer. Oncotarget. 2017;8:69756–67.
17. Sun W, Yan C, Jia S, Hu J. Correlation analysis of peripheral DPYD gene polymorphism with 5-fluorouracil susceptibility and side effects in colon cancer patients. Int J Clin Exp Med. 2014;7:5857–61.
18. Maletzki C, Huehns M, Knapp P, Waukosin N, Klar E, Prall F, et al. Functional characterization and drug response of freshly established patient-derived tumor models with cpg island methylator phenotype. PLoS ONE. 2015;10:e0143194.
19. Maletzki C, Stier S, Gruenert U, Gock M, Ostwald C, Prall F, et al. Establishment, characterization and chemosensitivity of three mismatch repair deficient cell lines from sporadic and inherited colorectal carcinomas. PLoS ONE. 2012;7:e52485.
20. Muller MF, Ibrahim AEK, Arends MJ. Molecular pathological classification of colorectal cancer. Virchows Arch. 2016;469:125–34.
21. Kuehn F, Mullins CS, Krohn M, Harnack C, Ramer R, Kramer OH, et al. Establishment and characterization of HROC69—a Crohn s related colonic carcinoma cell line and its matched patient-derived xenograft. Sci Rep. 2016;6:24671.
22. Hidalgo M, Amant F, Biankin AV, Budinská E, Byrne AT, Caldas C, et al. Patient derived xenograft models: an emerging platform for translational cancer research. Cancer Discov. 2014;4:998–1013.
23. El-Salhy M, Hilding L, Royson H, Tjomsland V. Comparison between triple therapy with octreotide, galanin and serotonin vs. irinotecan or oxaliplatin in combination with 5-fluorouracil/leukovorin in human colon cancer. Int J Oncol. 2005;27:687–91.
24. Dorsey JF, Mintz A, Tian X, Dowling ML, Plastaras JP, Dicker DT, et al. Tumor necrosis factor-related apoptosis-inducing ligand (TRAIL) and paclitaxel have cooperative in vivo effects against glioblastoma multiforme cells. Mol Cancer Ther. 2009;8:3285–95.
25. Kang HJ, Lee SH, Price JE, Kim LS. Curcumin suppresses the paclitaxel-induced nuclear factor-kappaB in breast cancer cells and potentiates the growth inhibitory effect of paclitaxel in a breast cancer nude mice model. Breast J. 2009;15:223–9.
26. Chang C-W, Liu C-Y, Lee H-C, Huang Y-H, Li L-H, Chiau J-SC, et al. *Lactobacillus casei* Variety *rhamnosus* probiotic preventively attenuates 5-fluorouracil/oxaliplatin-induced intestinal injury in a syngeneic colorectal cancer model. Front Microbiol. 2018;9:983.
27. Papanastasopoulos P, Stebbing J. Molecular basis of 5-fluorouracil-related toxicity: lessons from clinical practice. Anticancer Res. 2014;34:1531–5.

28. Gross E, Ullrich T, Seck K, Mueller V, de Wit M, von Schilling C, et al. Detailed analysis of five mutations in dihydropyrimidine dehydrogenase detected in cancer patients with 5-fluorouracil-related side effects. Hum Mutat. 2003;22:498.

29. Kleibl Z, Fidlerova J, Kleiblova P, Kormunda S, Bilek M, Bouskova K, et al. Influence of dihydropyrimidine dehydrogenase gene (DPYD) coding sequence variants on the development of fluoropyrimidine-related toxicity in patients with high-grade toxicity and patients with excellent tolerance of fluoropyrimidine-based chemotherapy. Neoplasma. 2009;56:303–16.

30. Dean L. Medical Genetics Summaries [Internet]. In: Pratt V, McLeod H, Rubinstein W, Dean L, Malheiro A, editors. *Fluorouracil therapy and DPYD genotype*. Bethesda, MD: National Center for Biotechnology Information; 2012. p. 2012–2016.

31. Roolf C, Richter A, Konkolefski C, Knuebel G, Sekora A, Krohn S, et al. Decitabine demonstrates antileukemic activity in B cell precursor acute lymphoblastic leukemia with MLL rearrangements. J Hematol Oncol. 2018;11:62.

32. Di Paolo A, Orlandi P, Di Desidero T, Danesi R, Bocci G. Simultaneous, but not consecutive, combination with folinate salts potentiates 5-fluorouracil antitumor activity in vitro and in vivo. Oncol Res. 2017;25:1129–40.

33. Lecomte T, Ferraz J-M, Zinzindohoue F, Loriot M-A, Tregouet D-A, Landi B, et al. Thymidylate synthase gene polymorphism predicts toxicity in colorectal cancer patients receiving 5-fluorouracil-based chemotherapy. Clin Cancer Res. 2004;10:5880–8.

34. Ostwald C, Linnebacher M, Weirich V, Prall F. Chromosomally and microsatellite stable colorectal carcinomas without the CpG island methylator phenotype in a molecular classification. Int J Oncol. 2009;35:321–7.